



Demand Risk in Arid Northwest China: More a result of 2 **Anthropogenic Activities than Climate Change** 3 Yang You¹, Pingan Jiang², Yakun Wang¹, Wene Wang¹, Dianyu Chen^{1,*}, Xiaotao Hu^{1,*} 4 5 1. Key Laboratory of Agricultural Soil and Water Engineering in Arid and Semiarid Areas, Ministry of Education, Northwest A&F University, Yangling 712100, China. 6 7 2. Xinjiang Agricultural University, Urumuqi 830052, China * Corresponding author: Dianyu Chen (dianyuchen@nwsuaf.edu.cn); 8 9 Xiaotao Hu(huxiaotao11@nwsuaf.edu.cn). 10 **Highlights:** 11 Irrigation water demand surge critically amplifies water supply-demand risk in arid 12 regions; 13 14 Water resources in arid regions are more susceptible to anthropogenic impacts; Regional water supply-demand risk continues to rise through the mid-21st century. 15 16 **Abstract** 17 Maintaining regional water supply-demand balance is crucial for achieving 18 sustainable development. Although the impacts of climate change and anthropogenic 19 20 activities on water resources are widely recognized, the dynamic response mechanisms of water supply-demand risk (WSDR) under their combined forcing remain unclear. 21 The Tailan River Basin (TRB), though situated in a typical arid climate zone, serves as 22 China's vital fruit and high-quality grain production base due to abundant solar-thermal 23 24 resources. However, systematic research on WSDR in this region is deficient, impeding guidance for healthy and stable development of large-scale farming. To address this, 25

Growth in Agricultural Water Demand Aggravates Water Supply-





we developed a WSDR analytical framework based on PLUS-InVEST models, 26 encompassing 24 climate-land change scenarios. This framework quantifies impacts of 27 climate change and anthropogenic activities on TRB's water supply-demand patterns 28 and associated risks. Results show that under the Balanced Economy-Ecology Strategy 29 30 (BES), effective land consolidation could add 531.2 km² of cultivated land by 2050. However, significant cultivated land expansion drives minimum water demand to surge 31 32 to 4.87×10⁸ m³, while maximum regional water supply reaches only 0.16×10⁸ m³, breaking the supply-demand balance. By 2050, the entire TRB will face WSDR crises, 33 34 with at least 46% of the region enduring endangered (Level III) risk. The root cause is persistent anthropogenic activities-particularly land-use change-triggering continuous 35 cultivated land expansion, increasing irrigation water demand and intensifying conflicts 36 37 between water demand and supply capacity. These findings underscore the need to deeply integrate multidisciplinary approaches within WSDR frameworks, in-depth 38 analysis of land-ecology-hydrology feedback mechanisms, to better address water 39 security challenges under climate change. This study can provide an important 40 41 scientific basis for the optimal allocation of regional soil and water resources and the sustainable development of agroecology. 42 Keywords: Climate change; Anthropogenic activities; Land use; Water supply-43 demand risk (WSDR); Sustainable water governance 44 45





Introduction

46

47

48

49

50

51

52

53

54

55

56

57

58 59

60

61 62

63

64

65

66 67

68

69

70

71 72

73

74

75

decades, intensified climate change (Carr et al., 2024), increased frequency of extreme weather events (Van et al., 2023), persistent population growth (Dolan et al., 2021), and lagging water management (Zhang et al., 2025c) have collectively accelerated global water depletion, leaving approximately 4 billion people under severe water scarcity (Mekonnen et al., 2016). Mismatches and mismatches between natural endowments of water resources and human needs in terms of spatial distribution and temporal variations further exacerbate regional water scarcity problems and failure to meet ecosystem and societal needs (Caretta et al., 2024). Projections indicate that over the next three decades, population growth, rising food demand, and accelerated urbanization will drive sustained increases in multisectoral water withdrawals particularly irrigation water (Flörke et al., 2018; He et al., 2021). The resulting surge in demand will lead to a chronic water deficit, posing a serious challenge to the achievement of the United Nations Sustainable Development Goals (SDGs), in particular SDG 6 (sustainable water management), SDG 7 (sustainable modern energy) and SDG 17 (sustainable use of terrestrial ecosystems) (Ma et al., 2025). Water resource surpluses and deficits are profoundly influenced by both climate change and human activities. Climate change deeply affects multiple key processes within the hydrological cycle, including changes in precipitation and evapotranspiration (Konapala et al., 2020). The AR6 Synthesis Report states that with every 0.5°C increase in global temperature, extreme heatwaves, heavy rainfall, and regional droughts become more frequent and intense (Mukherji et al., 2023), elevating the risks of extreme flooding (surplus) and drought (deficit). Research shows that changes in key climatic variables (precipitation, temperature, evapotranspiration) significantly perturb runoff, altering the availability of surface water resources. These changes also affect the biodegradation of soil organic matter and pollutants in rivers (Lipczynska et al., 2018), limiting the available water volume in river systems. The impacts of human

Water deficits (supply-demand gaps) are squeezing the viability of sustainable

water use and water security, exacerbating ecological vulnerability (Huggins et al.,

2022) and food security risks (Jones et al., 2024), particularly in arid zones. Over recent

77

78 79

80

81

82

83

84

85

86

87

88 89

90 91

92

93 94

95

96

97 98

99

100

101

102

103

104

105





activities on the global terrestrial hydrological cycle are also multifaceted. Human activities have altered 41% of the land surface cover, and this alteration can trigger changes in the ratio of evaporation to runoff (Bosmans et al., 2017). Furthermore, land use/cover change can significantly alter canopy interception, soil infiltration, and evapotranspiration, consequently exerting significant impacts on runoff volume and peak flow (Guo et al., 2020). It also severely affects critical watershed hydrological processes and soil moisture parameters (such as surface roughness, infiltration rate, soil structure, and hydraulic conductivity) (Patra et al., 2023). These alterations further affect processes such as precipitation infiltration, groundwater recharge, and soil water storage, ultimately impacting regional water resource availability. Beyond altering the natural water cycle, human activities also directly impact water supply and demand by modifying water use structure and intensity, thereby inducing positive or negative feedbacks on the water cycle and ecosystems (Boakes et al., 2024).

The impacts of climate change and human activities on water resources are not independent. Research indicates that the increase in runoff during the 20th century resulted from the combined effects of climate change and human activities, with the impact of human activities (specifically land cover change) even exceeding that of climate change in certain regions (Piao et al., 2007). Land use change can influence precipitation through alterations in surface energy balance, the water cycle, and largescale atmospheric circulation (Zhang et al., 2025a). Climate change catalyzes and amplifies the effects of land alteration by modifying the hydrological cycle, thereby altering meteorological elements and triggering more severe extreme disasters (floods and droughts). Furthermore, the relative influence of climate change versus human activities varies significantly across different environmental element. Studies show that climate change dominates the changes in runoff (Zeng et al., 2024), ecosystem services (Jia et al., 2024), and vegetation dynamics (Hu et al., 2025). Whereas, land use exerts a greater influence than climate change on terrestrial productivity (He et al., 2025), carbon use efficiency (Chen et al., 2024b), and soil variables (Ding et al., 2024). However, there is still a lack of systematic understanding regarding the relative contributions of climate change and human activities to water resource supply-demand





trends of supply-demand risks. Therefore, in-depth investigation into the response 107 mechanisms of water resource supply-demand balance and risks under the combined 108 effects of climate change and human activities constitutes a critical scientific problem 109 urgently requiring resolution. 110 Model prediction serves as a powerful tool for analyzing land use change, water 111 resource evolution processes, and changes in water supply and demand, among others. 112 The Patch-generating Land Use Simulation (PLUS) model, which integrates spatial, 113 empirical, and statistical models, can be used to accurately analyze land use change and 114 patch growth (Liang et al., 2021). Research demonstrates that PLUS outperforms many 115 other models in terms of simulation accuracy and captures the spatial characteristics of 116 land use change more realistically (Gao et al., 2022). The InVEST model excels in 117 allocating water resources and evaluating watershed water conservation functions, 118 119 among other applications, while also boasting advantages such as low data 120 requirements and strong spatial representation capabilities. Its water yield module has been widely applied and validated for water resource supply assessment across diverse 121 122 watersheds globally (Chen et al., 2024a; Ma et al., 2024). Coupling these two models (PLUS and InVEST) has been extensively applied in fields such as carbon storage 123 simulation, habitat quality assessment, and spatial optimization of ecosystem services 124 125 (Zhang et al., 2024; Huang et al., 2024; Wang et al., 2024b). However, the application of the coupled PLUS-InVEST model to deeply investigate the response mechanisms of 126 127 regional water supply and demand to the combined effects of climate change and human 128 activities remains limited (Gao et al., 2024). Water resources in arid regions are extremely scarce and their ecosystems are 129 highly fragile (Li et al., 2021), making them highly sensitive to both climate change 130 and human activities. Since 1980, cultivated land in China's arid regions has expanded 131 significantly by 25.87% (Zhu et al., 2021), profoundly impacting the allocation of water 132 and land resources and the ecological balance in these areas (Liu et al., 2025b). Under 133 the influence of climate change, both runoff (Li et al., 2025b) and precipitation (Yao et 134 al., 2022) have shown increasing trends, providing more available water resources for 135

balance, and how their interactions shape the spatial patterns and temporal evolution

137

138

139

140

141

142

143

144

145

146

147

148 149

150

151 152

153

154

155

156

157 158

159

160

161

162

163

164

165





continuous expansion of cultivated land has led to a surge in regional water use pressure, with irrigation water now constituting the primary consumptive portion of water Simultaneously, cultivated land expansion intensifies evapotranspiration (Zhu et al., 2025), and inefficient irrigation (with an irrigation water use efficiency coefficient of only 0.585 in Xinjiang) exacerbates groundwater overdraft (Yan et al., 2025) and soil salinization (Perez et al., 2024), continually intensifying the conflict between water supply and demand in arid regions. Although current research has focused on the individual impacts of climate change (Lu et al., 2024a; Hamed et al., 2024) and human activities (Zhu et al., 2023; Valjarević et al., 2022) on arid regions, there remains a lack of systematic investigation into the dynamic mechanisms of supply-demand risks driven by the coupling of these two factors. Therefore, within a comprehensive framework considering both climate change and human activities, it is necessary to quantify water supply-demand risks in arid regions and identify the key controlling factors, in order to support sustainable water management strategies for these areas. Based on this, we studied a typical watershed in the arid region of Northwest China, aiming to investigate water resource supply-demand balance under the influence of climate change and human activities, and to analyze the main influencing factors of water supply-demand risks. The specific objectives of this study are: i) To determine land change trends using the PLUS model under six development scenarios (NIS, FSS, EDS, WPS, EPS, and BES), and to identify the high-contribution factors driving land change. ii) To clarify the change processes of water supply and demand quantities under 24 land-climate combination patterns (resulting from four climate change scenarios and six land use change scenarios), and to analyze the key reasons driving these water supply-demand changes; iii) To quantify water supply-demand risks under the landclimate combination patterns, and to identify the main factors influencing these water supply-demand risks; iv) To propose practical management strategies and recommendations for water and land resource planning and allocation, and for agroecological sustainable development in typical arid region watersheds.

the region (Chen et al., 2023a). However, under the influence of human activities, the





2 Datasets and methods

2.1 Study Area

The Tailan River originates on the southern slope of Mount Tomur in the Tianshan Mountains. It is a typical inland river in the arid region of Northwest China (Fig. 1), primarily fed by glacial and snow meltwater, with a multi-year average runoff of 7.766×10⁸ m³. The Tailan River Basin (TRB) is composed of gravel, alluvial, and fine soil plains. It experiences a continental north-temperate arid climate, characterized by abundant sunshine and high evaporation. The multi-year average precipitation is 177.7 mm, evaporation is 2912 mm, air temperature is 8.6 °C, and wind speed is 1.25 m/s. The TRB is an important base for grain, cotton, oil crops, and fruits, having developed a diversified pattern centered on grain and cotton. It serves both as a trade hub for melons and fruits such as walnuts, apples, jujubes (red dates), and fragrant pears, and as a high-quality production area for important crops like cotton and rice.

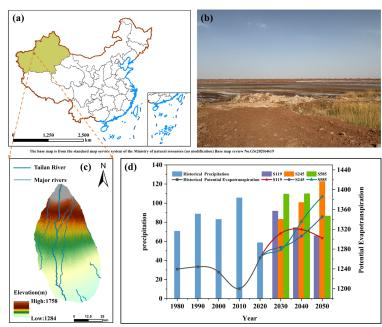


Fig. 1. Overview of the Tailan River Basin (TRB): (a) Schematic map showing the location of TRB in China; (b) Actual landscape of the Tailan River; (c) Digital Elevation Model (DEM) of TRB; (d) Precipitation and potential evapotranspiration for historical and future periods in TRB.





2.2 Datasets

183

184

185

186

187

188

189

190

191

192

193

194

195196

197

198199

200

This study collected two sets of datasets to simulate land use and water supplydemand in the TRB. The first set of data was used to simulate land use change (Tab. 1), involving a total of 19 factors influencing land use to establish a driving factor library. These include 10 socio-economic factors, 3 climate factors, 3 topographic factors, 2 soil factors, and 1 vegetation factor. The second set of data was used to simulate water supply and demand quantities, with a total of 12 factors employed for the simulation (Tab. 2). Additionally, land use and future climate were used as the base data, and land use data were obtained from RESDC (https://www.resdc.cn/), constructed using interactive visual interpretation methods based on Landsat MSS, TM/ETM and Landsat 8 images (Zhuang et al., 1999), which include cultivated land, forest land, grassland, water bodies, built-up land and unutilized land, with an overall accuracy of more than 95% (Liu et al., 2014). Future meteorological data were obtained from TPDC (https://www.tpdc.ac.cn/), and Coupled Model Intercomparison Project (CMIP6) was selected as the data source. Considering the size of the study area, modeling efficiency, and information richness, bilinear interpolation was employed to harmonize the spatial resolution of all datasets to 30 meters within the Krasovsky 1940 Albers coordinate

Tab 1. A table of factor bank depicting the factors driving land use change in Tailan River Basinstudy area

Category	Data	Year	Spatial Resolution	Source	
	Average annual precipitation	2000–2020		https://www.resdc.cn/	
Climatic	Average annual temperature		1000 m	nups.//www.resuc.cn/	
	Drought Index	2022		https://www.plantplus.cn/	
	Digital Elevation Model				
Terrain	Slope	-	30 m	https://www.gscloud.cn/	
	Slope direction		30 m		
Soil	Soil type	2009		https://www.fao.org/	





	Soil erosion	2019	1000 m	
Plant	Normalized Difference		20	1.44
	Vegetation Index		30 m	https://www.resdc.cn/
	Population	2010 2015 2020	100 m	https://hub.worldpop.org
	Gross Domestic Product	2010, 2015, 2020	1000 m	https://www.resdc.cn/
	Art Lorent Line		500	https://eogdata.mines.edu/p
	Nighttime lights		500 m	roducts/vnl/
G .	Distance to railway			
Socio-	Distance to highway			
economic	Distance to river system			
	Distance to primary road	2020	30 m	https://www.ngcc.cn/
	Distance to secondary road			
	Distance to township Road			
	Distance to residential areas			

000	TE 1 4	table of the	1 , 1 ,	11 /1	INTEGE	1 1
203	Ian / A	table of the	data lised to	n dive the	In V E S L 1	modille

Category	Data	Year	Source
CMID(Monthly precipitation		
CMIP6	Monthly temperature	2021–2100	https://www.tpdc.ac.cn/
(MRI-ESM2.0)	Monthly potential evapotranspiration		
G 11	Plant available water content	2000	https://www.fao.org/
Soil	Root restriction layer depth	2009	Yan (2020)
	Per-capita household water		
	consumption		77' '' T
	Water consumption per		Xinjiang Uygur Autonomous
g :	10,000 ¥ GDP	2000 2020	Region Water Resources
Socioeconomic	Per-hectare farmland irrigation	2000-2020	Bulletin
	consumption		
	GDP of Tailan River Basin		WenSu County and the Aksu
	POP of Tailan River Basin		City Statistical Yearbooks.





2.3 Methods

204

205

206207

208209

210

211212

213

The research approach of this study is to first predict land use change in the TRB under six scenarios for the period 2020-2050 and screen for the high-contribution drivers of land change in the TRB. subsequently predict the change processes of water supply and demand quantities in the TRB under 24 land-climate combination patterns for 2020-2050, and analyze the key drivers of these water supply-demand changes. finally quantify water supply-demand risks under the land-climate combination patterns, identify the main factors influencing these water supply-demand risks, and propose management and policy recommendations aligned with regional development. The framework and workflow of this research approach are illustrated in Fig. 2.

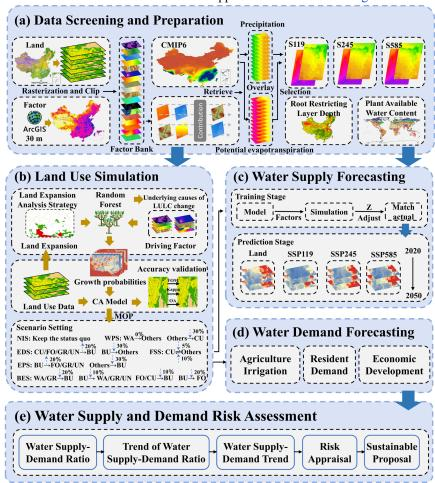


Fig. 2. Framework and Workflow for Multi-Scenario Water Supply-Demand Risk Assessment

216

217

218

219

220

221

222

223

224

225

226

227

228

229

230

231

232

233

234

235236

237

238

239

240

241

242

243

244





2.3.1 Land-Climate Model Setting

To explore the diverse possibilities for TRB's development, this study integrated the "Aksu Prefecture National Economic and Social Development 14th Five-Year Plan and Long-Range Objectives Through the Year 2035", the "Aksu Prefecture National Economic and Social Development Statistical Bulletin (2020-2024)", the "Aksu Prefecture Territorial Spatial Plan (2021-2035)", the "Xinjiang Uygur Autonomous Region Territorial Spatial Plan (2021-2035)", and previous research findings (Kulaixi et al., 2023; Song et al., 2025) to establish six land development scenarios. Natural Increase Scenario (NIS): Based on the land evolution process in the TRB from 2000 to 2020, this scenario maintains the current land transition processes, adds no new policy influences, and imposes no restrictions on the transfer probabilities between land use types. It serves as a baseline and reference for the other scenarios. It also functions as a control for observing transitions in the other restricted scenarios. Food Security Scenario (FSS): Based on the characteristics of the TRB region, this scenario emphasizes food security and enhances agricultural productivity. It reduces (by 5%) the transfer probability of cultivated land to other land use types while increasing (by 10%) the transfer probability from other land use types to cultivated land. Economic Development Scenario (EDS): Driven by accelerating urbanization and economic development needs, this scenario enhances economic construction and fundamental urban capacity. It increases (by 20%) the transfer probability from cultivated land, forest land, grassland, and unused land to built-up land, keeps the transfer probability from water bodies to built-up land unchanged, and simultaneously protects the TRB's economic infrastructure by reducing (by 30%) the probability of built-up land converting to other land use types except cultivated land. Water Protection Scenario (WPS): Addressing water scarcity and the need for aquatic ecological balance, this scenario prioritizes safeguarding ecological functions

Ecological Protection Scenario (EPS): Given the ecological fragility and

such as water resource protection and water conservation from infringement. It

prohibits the encroachment of existing water body areas by other land use types and

reduces (by 30%) the transfer probability from other land types to cultivated land.

246

247

248

249

250

251

252

253

254

255256

257258

259

260261

262

263

264

265

266267

268

269

270

271272

273

274





sensitivity of the TRB, this scenario aims to enhance the resilience of its ecoenvironment. It restricts (by 30%) the transfer probability from other land use types to built-up land and increases (by 20%) the transfer probability from built-up land to forest land, grassland, water bodies, and unused land. Balanced Economy and Ecology Scenario (BES): Responding to the dual demands of economic development and ecological governance in the TRB, this scenario seeks parallel development of urbanization and ecological conservation. It reduces (by 20%) the transfer probability from grassland and water bodies to built-up land, and reduces (by 10%) the transfer probability from cultivated land and forest land to built-up land. Building upon this, it reduces (by 20%) the transfer probability from built-up land to forest land, and reduces (by 10%) the transfer probability from built-up land to water bodies, grassland, and unused land. In response to the increasingly severe climate change, combining historical rainfall and potential evapotranspiration trends in the TRB (Fig. 1). this scenarios with Shared Socio-economic Pathways (SSP) and Representative Concentration Pathways (RCP) under CMIP6 were selected. While SSP describes possible future socio-economic developments, RCP depicts future greenhouse gas concentration and radiative forcing scenarios (O'Nill et al., 2016, 2017). Here, the typical SSP-RCP scenarios from the second-generation climate model (MRI-ESM2.0) as developed by the Meteorological Research Institute (MRI) of Japan were used. This includes: i) land, to compare current and future climate change; ii) SSP119, the lowest radiative forcing scenario with radiative forcing of ≈1.9 W/m² by 2100; iii) SSP245, a medium radiative forcing scenario that stabilizes at ≈4.5 W/m² by 2100; iv) SSP585, a high forcing scenario with

2.3.2 Land Use Projections

emissions rising to 8.5 W/m² by 2100.

This study employed the PLUS model to predict land use evolution trends in the TRB. The PLUS model consists of the Land Expansion Analysis Strategy (LEAS) and the CA based on multi-type random patch seeds (CARS) (Liang et al., 2021). The LEAS module utilizes the random forest algorithm to explore the relationships between multiple driving factors and different land types, thereby determining the development





potential for each land use type (Shi et al., 2023). The CARS module simulates patches of different land types by integrating a transition matrix and neighborhood weights of land use types to achieve the prediction outcome. In this study, the sampling rate of the random forest was adjusted to 0.2 and the number of decision trees was set to 60 to adapt to the geographical environment of the TRB. We selected the Figure of Merit (FOM), Overall Accuracy (OA), and Kappa index (Liu, et al., 2017) to measure the accuracy of the simulations. To enhance the applicability and precision of the PLUS model, the collected 19 driving factors were used as a 'factor bank'. Under consistent other simulation parameters, factors with lower contribution capabilities were systematically removed, and land use patterns for both 2015 and 2020 were simulated. Driving factors were screened based on the random forest algorithm within the LEAS module and the evaluation metrics. When the number of driving factors was reduced to 13, the simulation achieved the highest accuracy (Tab. 3) and exhibited strong consistency (Fig. 3). Consequently, this study adopted these 13 driving factors for subsequent simulations.

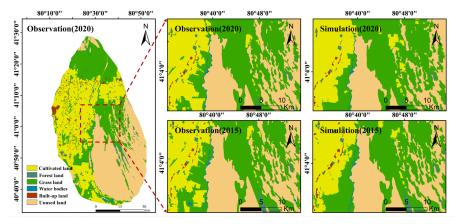


Fig. 3. Observed (2015/2020) and simulated land use maps of the Tailan River Basin (left/middle and right, respectively).

Table 3. Accuracy metrics of the PLUS model during different validation periods.

Simulation time	Number of factors	OA	Kappa	FOM
2015	7	0.91	0.86	0.17

295

296

297

298299

300

312

313

314





	13	0.92	0.88	0.18
	19	0.91	0.87	0.18
	7	0.88	0.83	0.19
2020	13	0.90	0.85	0.25
	19	0.85	0.85	0.24

2.3.3 Water Supply and Demand Forecasting

(1) Water Supply Forecasting

This study utilized the water yield module of the InVEST model to predict changes in water yield within the TRB (Tailan River Basin). The Budyko framework (Budyko, et al., 1974) was applied to determine the difference between precipitation and actual evapotranspiration for each grid cell, which was then used to calculate water yield (Chen, et al., 2024). The calculation formula is as follows:

301
$$Y_{(x)} = \left(1 - \frac{AET_{(x)}}{P_{(x)}}\right) \times P_{(x)}$$
 (1)

where $Y_{(x)}$ is the annual water yield of grid cell x; AET $_{(x)}$ is the actual evapotranspiration in grid cell x; and $P_{(x)}$ is the annual precipitation in grid cell x. Evapotranspiration of vegetation under the various land use types was calculated (i.e., $\frac{AET}{P_{(x)}}$) after Zhang et

305 al. (2004) as follows:

306
$$\frac{AET_{(x)}}{P_{(x)}} = 1 + \frac{AET_{(x)}}{P_{(x)}} - \left[1 + \left(\frac{PET_{(x)}}{P_{(x)}}\right)^{\omega}\right]^{1/\omega}$$
 (2)

where $PET_{(x)}$ is the potential evapotranspiration (mm) of grid cell x, and ω is an empirical value related to natural climate and soil properties. The term $\omega(x)$ is calculated after Donohue (2012) as:

310
$$\omega(x) = Z \frac{AWC_{(x)}}{P_{(x)}} + 1.25 \tag{3}$$

311
$$AWC_{(x)} = min(MaxSoilDepth_{(x)}, RootDepth_{(x)}) \times PAWC_{(x)}$$
 (4)

where Z is a seasonal constant of the water yield model, representing hydrogeological characteristics such as regional precipitation distribution. Based on "the Wensu County Water Resources Development Plan for the 14th Five-Year Plan Period" and "the





Comprehensive Report on the Tailan River Basin Planning", the surface water resources volume in the plain area was determined to be 65×10^5 m³. Through manual optimization, it was found that when the model parameter Z = 7.5, the discrepancy between the simulated and observed values was minimized (Fig. 4).

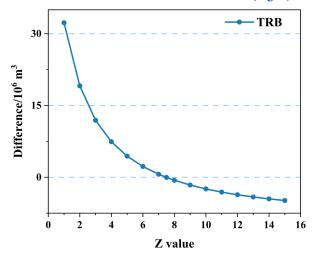


Fig. 4. Discrepancy between observed and simulated surface water resources volume in the Tailan River Basin under different Z values.

AWC_(x) is the effective water content of grid cell x; PAWC_(x) is the effective water content of vegetation in grid cell x; MaxSoilDepth_(x) is the maximum soil depth in grid cell x; and RootDepth_(x) is the root depth in grid cell x. The term PAWC_(x) is as follows (Zhou et al., 2005):

325
$$PAWC_{(x)} = 54.509 - 0.132SAND_{(x)} - 0.003(SAND_{(x)})^{2} - 0.055SILT_{(x)}$$
326
$$-0.006(SILT_{(x)})^{2} - 0.738CLAY_{(x)} + 0.007(CLAY_{(x)})^{2}$$
327
$$-2.699OM_{(x)} + 0.501(OM_{(x)})^{2}$$
(5)

where SAND(x), SILT(x), CLAY(x), and OM(x) respectively stand for sand, silt, clay, and organic matter contents of grid cell x.

(2) Water Demand Forecasting

As indicated by "the Wensu County Statistical Bulletin on National Economic and Social Development" and "the Aksu Statistical Bulletin on National Economic and Social Development", the water use structure in the TRB (Tailan River Basin) is well-

335

336

337

338

339

340

341

344

345

346 347

348

349 350

354

355

356

357

358 359

360 361

362





defined, primarily sourced from agricultural irrigation, residential consumption, and economic development activities. Therefore, this study conducted separate projections for agricultural water demand, domestic water demand, and economic water demand within the TRB. In order to account for the impact of climate change on the average crop water requirement in the TRB, and based on the findings of Li et al. (2020), which indicate that a temperature increase of 2 °C leads to an increase in the average crop water requirement of 19 mm, the formula for calculating irrigation water demand per hectare was derived as follows:

$$\Delta cwd_{(a,b)} = 9.5 \times (T_2 - T_1) \tag{6}$$

$$n_{(a,b)} = d_0 + \Delta cw d_{(a,b)} \tag{7}$$

where $\Delta cwd_{(a,b)}$ represents the change in average crop water requirement for grid cell b in year a, T1 denotes the air temperature for a grid cell during the baseline period, and T2 denotes the air temperature for the same grid cell during the change period. n_(a,b) is the irrigation water demand per hectare for grid cell b in year a under climate change impacts, and do is the irrigation water demand per hectare during the baseline period. Therefore, the calculation formulas for agricultural water demand, domestic water demand, and economic water demand are as follows:

351
$$pop_{(a,b)} = \frac{p_{(a,b)}}{\sum_{b=1}^{n} p_{(a,b)}} \times POP_a$$
(8)
$$gdp_{(a,b)} = \frac{g_{(a,b)}}{\sum_{b=1}^{n} g_{(a,b)}} \times GDP_a$$
(9)

352
$$gdp_{(a,b)} = \frac{g_{(a,b)}}{\sum_{b=1}^{n} g_{(a,b)}} \times GDP_a$$
 (9)

353
$$WD_{(a,b)} = pop_{(a,b)} \times l_{(a,b)} + gdp_{(a,b)} \times m_{a(a,b)} + agr_{(a,b)} \times n_{(a,b)}$$
(10)

where $p_{(a,b)}$ and $g_{(a,b)}$ are respectively the initial population and economic status of grid cell b in year a; POP_a and GDP_a are respectively the population and GDP in year a; $pop_{(a,b)}$ and $gdp_{(a,b)}$ respectively the calibrated population and GDP of grid cell b in year a; and $agr_{(a,b)}$ is the cultivated land area of grid cell b in year a. the terms l_a , m_a , and n_a respectively represent the per capita water use, water use per 10,000 Yuan of GDP, and irrigation water use per hectare of farmland in year a. To exclude recharge from the mountain in the study area, the amount of surface water resources in the mountains was equally dispersed in a raster. The population and GDP for 2030-2050 were determined using linear regression method. To exclude the water contribution

364

365

366

367

368

369

370

371

372

373374

375376

377

378

379

383

384

388 389





from the upper reaches of the Tailan River to this study, the multi-year average runoff from the upper reaches was evenly allocated to each grid cell to reduce its influence on water demand calculations. Additionally, this study employed linear regression to project the population and GDP for the period 2030–2050, which was used to support the prediction of the temporal change in water demand within the TRB from 2030 to 2050.

2.3.4 Risk Framing of Water Supply and Demand

The water supply-demand risk framework serves as a crucial tool for assessing regional water supply-demand risks. Moran (2017) classified the computational results generated within this framework into seven categories (Tab. 4), enabling the assessment of regional water risk levels by calculating the water supply-demand relationship and facilitating the quantification of regional water supply-demand risk grades. This framework comprises four indicators: the water supply-demand ratio, the trend in the water supply-demand ratio, the water supply trend, and the water demand trend. The calculation procedures for these indicators are as follows:

1) The water supply and demand ratio that expresses spatial heterogeneity of water supply and demand contradictions:

$$R_{(x)} = WY_{(x)} / WD_{(x)}$$
 (9)

where $R_{(x)}$ is the water supply-demand ratio of grid cell x; and $WY_{(x)}$ and $WD_{(x)}$ are respectively the water supply and demand of grid cell x.

2) The trend of water supply-demand ratio expresses the relative changes in water supply and demand:

$$R_{tr} = R_i - R_i \tag{10}$$

where R_{tr} is the difference between water supply-demand ratios in years i and j; R_i and R_i are respectively the water supply-demand ratios in years i and j.

3) The trend of water supply and demand volume expresses the absolute changes in water supply and demand volume:

$$S_{tr} = WY_i - WY_i \tag{11}$$

$$D_{tr} = WD_i - WD_j \tag{12}$$

where S_{tr} and D_{tr} are respectively the differences in water supply and demand volumes;





393 WY_i and WY_j respectively the water supply volumes in years i and j; WD_i and WD_j

respectively the water demand volumes in years i and j.

395 Table 4. Assessment of water supply and demand risk level in the study area

Grade code	Risk grade	Water supply-demand ratio (R)	Water trend of supply-demand ratio (R _{tr})	Trend of water Supply (S _{tr}) and demand (D _{tr})
I	Extinct/ Dormant	R = 0	$R_{tr} < 0$	_
II	Critically endangered	0 < R < 1	$R_{tr} < 0$	$S_{tr}\!<\!0,D_{tr}\!\ge\!0$
III	Endangered	0 < R < 1	$R_{tr}\!\ge\!0$	$\begin{split} S_{tr} &< 0, D_{tr} < 0 \text{ or} \\ S_{tr} &\geq 0, D_{tr} \geq 0 \end{split}$
IV	Dangerous	0 < R < 1	$R_{tr}\!\ge\!0$	$\begin{split} S_{tr} &< 0, D_{tr} < 0 \text{ or} \\ S_{tr} &\geq 0, D_{tr} \geq 0 \end{split}$
V	Undersupplied	0 < R < 1	$R_{\rm tr} < 0$	$S_{tr} \geq 0, \ D_{tr} < 0$
VI	Vulnerable	$R \ge 1$	$R_{tr} \geq 0$	_
VII	Safe	$R \ge 1$	$R_{tr}\!\geq 0$	_

396 3 Results

3.1 Spatial heterogeneity of land use to multi scenario

The evolution of land use in the TRB from 2020 to 2050 under six scenarios was simulated using the PLUS model. Overall, the land use structure remained relatively stable across the multiple scenarios, with the most significant changes primarily manifested in cultivated land and grassland areas (Fig. 5). Notably, grassland area generally exhibited significant degradation (with an average reduction of 535.36 km²), whereas cultivated land area expanded substantially due to factors such as policy incentives and population growth (with an average increase of 524.87 km²). Under the NIS, the intensity of cultivated land reclamation continuously increased, with its proportion jumping from 33% (2020) to 46% (2050). A significant portion of this expansion stemmed from the reclamation of grassland. Simultaneously, the encroachment of built-up land also constituted a major component of grassland conversion. Compared to NIS, the FSS resulted in a greater expansion of cultivated land (545.28 km²). This scenario emphasizes intensive land use and promotes sustainable cultivated land development through the consolidation of fragmented farmland. The cultivated land expansion under FSS primarily originated from the conversion of

414

415

416

417

418

419

420

421

422

423

424

425 426

427

428

429

430

431





grassland. Under the EDS, the area of built-up land surged from 62.88 km² (2020) to 113.05 km² (2050), significantly exceeding that in other scenarios. Urban expansion primarily encroached upon cultivated land and grassland (Liu et al., 2015). Relative to NIS, the WPS mitigated grassland reclamation and degradation, increased water conservation and ecological land, and augmented grassland area through soil conservation measures and the development of wasteland. Building upon WPS, the EPS further restricted human activities, resulting in the smallest built-up land area (104.08 km²). While controlling the growth rate of cultivated land area, it significantly increased the area of ecological land, such as grassland and water bodies, thereby further restoring the fragile ecosystems in the arid region. As a key measure to balance ecology and economy in the arid oasis region, the BES maintained a relatively high cultivated land area (531.20 km²) to safeguard the agricultural economic backbone. Simultaneously, it ensured that ecological land, such as woodland and water bodies, remained free from encroachment. Furthermore, it involved further development of unused land (wasteland and saline-alkali land), converting it into grassland (31.08 km²) with ecological conservation functions.

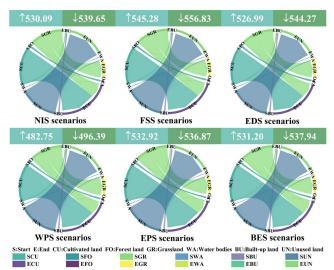


Fig. 5. Transfer process under six land-use scenarios in the Tailan River Basin, 2020–2050 (Scenario labels indicate cultivated land expansion area (blue; in km²) and grassland degradation area (green; in km²)).





Different land types exhibit significantly varying degrees of responsiveness to driving factors due to differences in their spatial demand and evolutionary trajectories (Fig. 6). Specifically, population plays a core driving role in the evolution of multiple land types: it exhibits the highest contribution rates to cultivated land (0.20), forest land (0.19), grassland (0.17), built-up land (0.18), and unutilized land (0.43). Other key driving factors also show specific influences: the Nighttime Light Index has relatively high contributions to cultivated land (0.12) and built-up land (0.29), the Aridity Index to forest land (0.11) and grassland (0.09), and the Digital Elevation Model (DEM) also contributes significantly to water bodies (0.38).

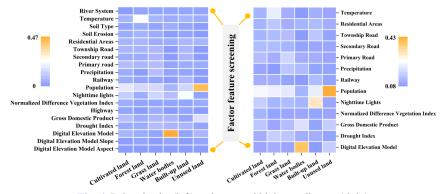


Fig. 6. Driver banks (left) and screened high contributors (right)

3.2 Multi-Scenario Water Supply-Demand Dynamics

(1) Variation in water supply

Based on the InVEST model, the variation trends of water supply under different climate change and land use scenarios were investigated. The spatial distribution of water resources supply remains consistent across scenarios, with a stable water supply pattern (Fig. 7a). This pattern demonstrates significantly higher water supply in the northern region than elsewhere, which is closely linked to the spatial distribution of precipitation in the TRB. During 2020-2050, water supply trends under different scenarios show distinct variations: both Land and S245 exhibit an upward trend, with S245 increasing at a significantly faster rate than land. In contrast, the water yield capacity of S119 and S585 gradually declines over time, though their decreasing trends differ substantially (Tab. 5). Furthermore, the contribution of water yield capacity from



455

456

457

458

459

460

461



different land types to water supply also varies, with grassland providing significantly higher water supply than cultivated land. Using the scenario maintaining current rainfall and potential evapotranspiration (Land) as the baseline, TRB's water supply fluctuates under different land use scenarios, ranging from 64.78×10^5 m³ to 65.7×10^5 m³. Under different climate scenarios, TRB's water supply shows pronounced variations, with a fluctuation range of 25.33×10^5 m³ to 162.2×10^5 m³ when referenced against the NIS baseline scenario. The highest water supply in TRB (162.8×10^5 m³) occurs under the S245-FSS, while the lowest (25.23×10^5 m³) is observed under the S119-EPS.

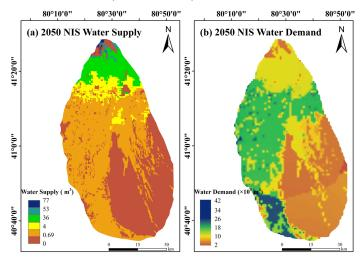


Fig. 7. Spatial patterns of water supply (a) and water demand (b) in the Tailan River Basin for 2050
 Table 5. Dynamics of Water Supply and Demand in the Tailan River Basin Under 24 Land-Climate

464 Combination Scenarios (2020–2050)

Year		Water yield supply(×10 ⁵ m³)							Water yield demand(×10 ⁵ m³)					
		NIS	FSS	EDS	WPS	EPS	BES	Year	NIS	FSS	EDS	WPS	EPS	BES
202	20		64.68				2020	158.98						
	2030	64.78	64.92	64.60	64.53	64.99	64.93	2030	1887	1993	1879	1575	1899	1892
LAND	2040	64.94	65.17	64.83	64.79	65.32	65.05	2040	3448	3535	3440	3188	3461	3453
	2050	65.70	65.59	65.59	65.67	65.46	65.69	2050	4865	4935	4850	4646	4878	4870
G110	2030	64.06	64.25	63.76	63.69	64.47	64.35	2030	2089	2198	2081	1769	2101	2094
S119	2040	32.49	32.64	32.41	32.37	32.75	32.58	2040	3667	3756	3659	3400	3680	3673

466

467 468

469

470

471

472

473

474

475

476

477

478

479

480

481

482

483

484 485

486





	2050	25.33	25.29	25.26	25.31	25.23	25.33	2050	5060	5132	5046	4837	5074	5066
	2030	51.05	51.19	50.80	50.76	51.37	51.27	2030	1997	2104	1989	1680	2009	2002
S245	2040	89.33	89.68	89.12	88.97	89.93	89.55	2040	3554	3642	3546	3291	3567	3560
	2050	162.2	162.8	162.6	162.5	162.3	162.7	2050	5269	5342	5254	5040	5283	5274
	2030	138.0	138.3	137.6	137.4	138.7	138.5	2030	2032	2141	2024	1715	2044	2038
S585	2040	133.5	133.9	133.1	133	134.3	133.8	2040	3749	3839	3740	3479	3762	3754
	2050	61.82	61.79	61.71	61.78	61.62	61.81	2050	5316	5390	5301	5086	5330	5321

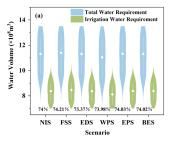
(2) Variation in water demand

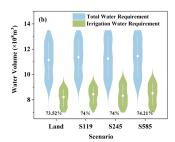
Compared with water supply, the spatial distribution and pattern of water demand also remain relatively consistent and stable across different scenarios (Fig. 7b) This pattern exhibits stronger water demand capacity in the southwestern and central-eastern regions but weaker capacity in the northern and southeastern areas, which is closely associated with the spatial distribution of land use and population aggregation density in the TRB. During 2020-2050, water demand under all scenarios shows a continuous upward trend, though with significant variations in the rate of increase. Furthermore, the contribution of water demand capacity from different land types varies markedly, with cultivated land and built-up land demonstrating stronger demand capacity, while unutilized land shows the weakest capacity. Using the scenario maintaining current rainfall and temperature (Land) as the baseline, TRB's water demand exhibits significant variations under different land use scenarios (Tab. 5), ranging from 1575 × 10⁵ m³ to 4935 × 10⁵ m³. Under different climate scenarios, TRB's water demand displays similar upward trends over time, with a fluctuation range of 1887 × 10⁵ m³ to 5316×10^5 m³ relative to the NIS baseline scenario. The highest water demand (5390 \times 10⁵ m³) occurs under the S585-FSS scenario, whereas the lowest (1575 × 10⁵ m³) is observed in the Land-WPS scenario. Agricultural water use has consistently constituted the primary consumption component in the TRB. Across all land and climate change scenarios, irrigation accounts for over 70% of the total share (Fig. 8a, b). Although the proportion of irrigation water gradually decreases over time, its total volume continues to increase (Fig. 8c). Nevertheless, unilateral studies of water supply or demand alone





cannot directly reflect water resource allocation capacity. The impacts arising from supply-demand imbalances remain unclear and warrant further investigation. To better elucidate the impacts of water supply-demand dynamics on TRB's water resources, indepth analysis of regional water security risks is required, which will facilitate the formulation of tailored water management and conservation strategies.





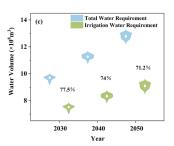


Fig. 8. Dynamics of total water demand and agricultural irrigation demand with proportional distribution across latitudinal gradients in the Tailan River Basin, 2030–2050(a) Different land change scenarios; (b) Different climate change scenarios; (c) Temporal evolution.

3.3 Multi-Scenario Water Supply-Demand Risks and Attribution

To assess water supply-demand risks in the TRB region, an evaluation framework was established using four indicators: water supply-demand ratio, trend of water supply-demand ratio, water supply trend, and water demand trend. Spatial patterns of water supply-demand risk in the TRB exhibit heterogeneity across scenarios (Fig. 9). Under identical climate change scenarios, risk variations across land use scenarios are insignificant, with consistent spatial distribution of risk classification levels. This consistency arises from unchanged rainfall and potential evapotranspiration patterns. Although risk classification levels vary under different climate scenarios, no grid cell in the TRB escapes hazardous (Level IV) risk (Tab. 3 indicates a 7-level classification system). This is closely linked to continuously increasing water demand in the TRB. Using NIS as the baseline, the scenario maintaining current rainfall and potential evapotranspiration (Land) shows the most severe water scarcity: Level II risk accounts for 51.31%, while Level IV risk constitutes merely 0.85%. Under the other three climate scenarios, water supply-demand risks are alleviated, with Level IV risk proportions being 29.24% (S119), 53.60% (S245), and 49.34% (S585) respectively (Fig. 10). The

512

513514

515

516517

518

519

520





S245-EPS scenario achieves maximum risk mitigation in the TRB, as its rainfall levels increase steadily per decade among the three climate scenarios (Fig. 1d), thereby alleviating regional water stress. While the TRB's harsh current climate exacerbates water risks, future climatic changes may moderately alleviate these risks compared to present conditions. In summary, by 2050 the entire TRB will face water supply-demand crises, with at least 46% of the area subjected to endangered (Level III) risk, including no less than 10% of land confronting critical endangered (Level II).

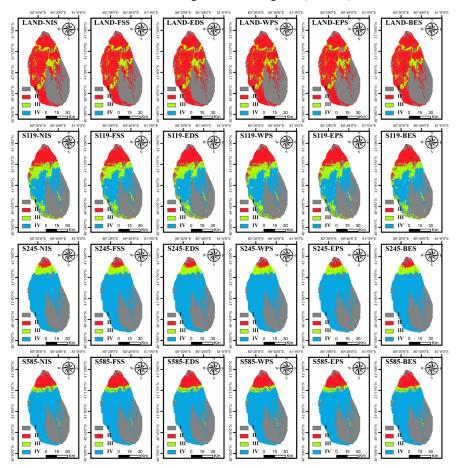


Fig. 9. Spatial evolution of water supply-demand risk classification levels in the Tailan River

Basin (TRB) under 24 climate-land combination scenarios (2020–2050)

(Color gradient indicates decreasing risk from Level I (highest) to Level VII (lowest))





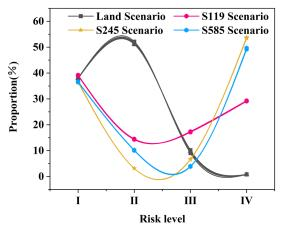


Fig. 10. Temporal variation in proportional distribution of risk classification levels across the Tailan River Basin (TRB) under 24 climate-land combination scenarios (2020–2050) (decreasing risk from I to VII)

4 Discussion

521

522

523

524

525526

527

528529

530531

532

533

534535

536

537

538

539

540541

4.1 Multi-Scenario Land Use Spatial Patterns

The selection of land use patterns determines the spatial layout and functions of urban systems (Zhao et al., 2021), serves as a fundamental element for territorial spatial planning and configuration (Chen et al., 2023b), and constitutes a critical approach to optimizing regional spatial structure, coordinating development processes, and achieving ecologically-economically synergistic sustainability within limited resources and space (Feng et al., 2025; Wu et al., 2025). In this study, the FSS adopts a more cohesive evolution trajectory for cultivated land (Fig. 5), exhibiting high intensification and contiguity (1937.58 km²). As an important economic driver in the TRB, the sustained rapid expansion of cultivated land will directly stimulate regional agricultural development, indicating that human activities determine land use trajectories and patterns. However, due to challenges in saline-alkali land remediation, cultivated land expansion encroaches on additional grassland, which will induce severe ecological degradation. The EDS further amplifies human impacts on land use, exacerbating compression for grassland (682.84 km²). Chen et al. (2023) demonstrates that ecological degradation from urbanization parallels that from cultivated land expansion, while more intensive human activities in urbanized areas may inflict greater ecological





damage. This implies that under anthropogenic pressure, heightened agricultural intensification and settlement land demand encroach upon more ecological land (forest and grassland), generating increased ecological deficits. The WPS strengthens ecological barriers by curbing agricultural land expansion and restricting grassland conversion, thereby reducing water resource consumption. Building on this, the EPS mitigates land fragmentation by controlling built-up land growth rates. Results indicate both WPS and EPS decelerate grassland degradation. This reveals that anthropogenic resource consumption rates substantially exceed natural recovery rates, with their antagonistic relationship weakening as human activities intensify. To maintain antagonistic equilibrium, the BES appropriately reduces cultivated land and built-up land areas, alleviating human encroachment on grassland (689.17 km²). It represents a prioritized model for future decision-making. Diverse land use scenarios reflect regional policy orientations and latent conflicts (Qi et al., 2025). Significant spatial heterogeneity necessitates targeted land management strategies to mitigate future anthropogenic impacts on natural ecosystems.

Results from Table 3 reveal that increasing the number of driving factors does not necessarily improve outcomes. Although random forests can effectively handle multicollinearity among factors, complex correlations and interactions between driving factors may still compromise simulation accuracy (Liang et al., 2021). Specifically, utilizing 13 core driving factors yields optimal simulation performance. Adding factors with low contribution rates beyond this threshold disturbs patch simulation directionality and quantity, thereby reducing precision. Conversely, reducing the number to 7 significantly degrades simulation quality, indicating high sensitivity of the PLUS model to feature factors. The absence of key drivers directly impairs patch simulation accuracy. Significant disparities in factor contribution rates (Fig. 6) demonstrate that human activity intensity and population distribution density govern land evolution processes. Shifts in population size trigger changes in affluence levels and food calorie demand, generating cascading effects on land resources, agroecosystems, and water resources (Beltran et al., 2020; Harifidy et al., 2024).

573

574

575

576

577

578

579

580 581

582

583

584 585

586

587 588

589

590 591

592

593594

595

596

597

598

599

600

601





4.2 Land Use and Climate Change Impacts on Water Supply-Demand Dynamics

(1) Impacts of Climate Change and Land Use on Water Supply

Water supply in the TRB is jointly constrained by human activities and climate change. Under the same climate change conditions, there are differences in water supply between different land use scenarios, and these differences are caused by different land use structures (Jia et al., 2022). Different geographical and climatic environments, as well as land surface, soil, and vegetation conditions, all affect water yield capacity (Fig. 7). However, its range of fluctuation is much lower than that of different climate change scenarios, indicating that climate change (precipitation) has a more significant impact on TRB water supply than human activities (land use change) (Luo et al., 2025). Because precipitation change is the decisive factor driving interannual water supply variation (Zhang et al., 2025b), water yield capacity is highly sensitive to rainfall levels (Shirmohammadi et al., 2020). Significantly similar trends between rainfall and water supply have been found in 17 typical Chinese basins (Guo et al., 2023), and this has also been validated in multiple watersheds in Argentina (Nuñez et al., 2024), the Gulf of Mexico Basin (Ouyang et al., 2025), and the United States (Duarte et al., 2024). In our study, precipitation and water supply also showed similar trends. In arid regions, there is a clear correlation between water supply and rainfall, and precipitation can explain most of the water supply variation (Adem et al., 2024). Notably, water supply in humid areas is more sensitive to rainfall changes than in arid areas. Therefore, water scarcity issues in arid regions require greater attention (Taylor et al., 2019).

(2) Impacts of Climate Change and Land Use on Water Demand

Water demand in the TRB is also constrained by both human activities and climate change. Under the same land use scenario, water demand varies across different climate scenarios, with this variation driven by temperature-induced changes in irrigation water use (Li et al., 2020). However, climate change impacts on water demand are substantially lower than those from land use changes (Table 5), indicating that human activities (land use) exert a more significant influence on TRB water demand than climate change. It is clear that irrigation water consumption accounts for the majority

603

604

605

606

607

608

609

610

611

612613

614 615

616

617618

619620

621

622

623 624

625

626

627

628

629

630

631





of TRB water consumption (Fig. 8). Changes in TRB's irrigation water are closely linked to (1) conversions between cultivated land and other land types, and (2) adjustments in planting patterns within cultivated areas. Studies demonstrate that volatile land allocation significantly affects agricultural irrigation, particularly through land type conversions (Cao et al., 2024). Simultaneously, land fragmentation levels influence water user numbers, while changes in irrigated area and frequency intensify irrigation water pressure (Sharofiddinov et al., 2024). This indicates that expanding cultivated land areas drive increased irrigation water usage (Liu et al., 2025a), aligning with our findings. Additionally, planting area and planting structure significantly impact irrigation water use (Chen et al., 2020). Sun et al. (2024) confined irrigation water within manageable levels while boosting yield and carbon sequestration by adjusting rice, maize, and soybean cultivation areas; Other research reduced irrigation water by 34.48% while decreasing crop greenhouse gas emissions by 10% through planting structure optimization (Li et al., 2025a). Moreover, interactions between irrigation technology and planting structure adjustments affect irrigation demand. Wu et al. (2024) found that combining deficit irrigation with high-density planting reduces irrigation water by 20% without compromising cotton yield. Furthermore, growers' strong traditional agricultural values make produce value and labor costs more critical concerns than irrigation water consumption (McArthur et al., 2017; Nourou et al., 2025). For instance, widespread maize cultivation (an economic crop) in the TRB substantially increases regional irrigation water volumes (Huang et al., 2015). Consequently, adjusting regional cropping structures within a macro-agricultural framework is crucial for ensuring sustainable water use and safeguarding growers' economic returns. Climate change and human activities exert non-singular impacts on water resources (Tan et al., 2025). Concurrently, variations in water supply and demand are jointly influenced by both factors (Tian et al., 2025). Precipitation affects the Normalized Difference Vegetation Index (NDVI) and Net Primary Productivity (NPP), subsequently altering crop phenology and water requirements, which induces changes in underlying surface land types (grassland, forest, and cultivated land). This cascade

633

634

635

636

637

638639

640

641

642643

644 645

646

647648

649

650

651

652653

654

655

656

657

658

659

660

661





alters watershed runoff generation/concentration and evapotranspiration, ultimately feeding back to precipitation. This demonstrates complex interactive feedback mechanisms between climate change and land use (Qi et al., 2025). Under these mechanisms, distinct climate scenarios yield significantly different water supplies. However, the magnitude of water supply variation (137.47 \times 10⁵ m³) remains substantially smaller than water demand variation (3815 \times 10⁵ m³). This indicates that human activities exert a far greater influence on water resources in the TRB than climate change.

4.3 Land Use and Climate Change Impacts on Water Supply-Demand Risks

By mid-century, water resource vulnerability in the TRB will be profoundly impacted by climate change and human activities. Global parallels exist: Lu et al. (2024b) demonstrated under multiple land-climate scenarios that synergies between crop production and water yield requirements increase agricultural output but exacerbate water deficits. Chen et al. (2023) documented significant oasis expansion in China (1987-2017), where increased precipitation and runoff provided partial compensation, yet climate-land changes substantially altered regional water supply. Gaines et al. (2023) found forest cover crucial for maintaining consistent surface water areas across climate-land cover scenarios. These findings confirm that climate change and human activities jointly govern water supply and demand. In our risk assessment framework, water demand trends consistently register negative values (<0), indicating persistent demand growth. This stems from cultivated land expansion driving rising irrigation needs, aligning with prior reports (Qi et al., 2025). Although agriculture water demand share of total water demand declines during 2020-2050, it remains dominant (70%) (Fig. 8). This correlates directly with Section 4.2 findings: (1) conversions between cultivated land and other land types, and (2) adjustments in planting patterns within cultivated areas. Crucially, the arid TRB's limited rainfall cannot meet growing irrigation demands, elevating water risk (Land scenario). Compared to current rainfall, three other climate scenarios increase precipitation (2020-2050), improving supply and moderately reducing water supply-demand risk (Fig. 9-10). Nevertheless, supplydemand gaps persist at nearly two orders of magnitude, with all areas remaining in

663

664

665

666

667

668

669

670

671

672673

674 675

676

677678

679680

681

682

683 684

685

686

687

688

689

690

691





"hazardous (Level IV) risk". Thus, human activities remain the primary driver of TRB's water supply-demand risks. Human activities dominate multiple dimensions within these climate-human interactions. Wang et al. (2025) identified human withdrawals as the key driver of reduced runoff and dampened seasonal variability in the Wei River Basin. Similarly, human exceed climate effects on soil moisture decline in China's monsoon loess critical zone (Wang et al., 2024a). Therefore, amid increasing uncertainty, integrating multi-method approaches within water risk frameworks to decipher land-eco-hydrological feedbacks, quantify risks, implement preemptive water regulations, and minimize secondary disasters to ecosystems and societies is imperative.

4.4 Limitations and recommendations for future research

Nevertheless, this study has several limitations. (1) Using land change as the starting point, we incorporated multiple drivers for land change simulation. Although our scenario design referenced the TRB's future spatial planning, we did not quantify its impact on urban construction. This may constrain in-depth exploration of land type conversions. Despite screening out drivers with low contribution rates, the influence of TRB's unique geographical setting and ecological processes on land conversion warrants further investigation. Future research could quantify territorial planning and government policies to examine eco-climatic-environmental impacts on land use transitions in arid regions. (2) We employed the InVEST model for water yield simulation, using 24 climate-land scenarios to reduce uncertainties in TRB's development trajectory. The Biophysical Table in the water yield module utilized FAO's "Crop Evapotranspiration: Guidelines for Computing Crop Water Requirements" (https://www.fao.org/) and research findings (Yan et al., 2022). However, over-reliance on precise parameters for evapotranspiration coefficients and root depths introduces uncertainties, given the dynamic nature of crop growth and water demand processes. Subsequent studies could integrate long-term crop observation data and crop models based on clarified regional planting structures to refine parameters and reduce uncertainties.

Located in an arid oasis region, water resources constitute the lifeline for human activities and ecosystems in the TRB. However, the arid and rain-scarce climate of TRB

693

694

695

696

697

698

699

700

701

702

703

704705

706

707

708

709710

711

712

713714

715

716

717

718 719

720

721





has led to a continuous amplification of the impact of human activities on the ecological environment, with irrigation water demand escalating daily (Chen et al., 2023a; Zhu et al., 2025). Concurrently, human survival necessitates improved living standards and economic development, intensifying human-land conflicts. Based on our findings, we recommend adopting the Balanced Economy and Ecology Scenario (BES) development model in the TRB, implementing diverse water-saving measures (sprinkler irrigation, subsurface drip irrigation, brackish water irrigation) to control water consumption (Han et al., 2022; Liang et al., 2024), thereby expanding cultivable land reserves.

5 Conclusions

Elucidating the impacts of climate change and human activities on water supplydemand risks is critical. We applied the PLUS model with six land change scenarios to identify suitable land development strategies for the TRB, and coupled it with the InVEST model under 24 climate-land scenarios to simulate dynamic changes in water supply and demand. Based on this, a water supply-demand risk framework was established to quantify TRB's water supply-demand risks during 2020-2050. Results show that the Balanced Economy and Ecology Scenario (BES) land development model promotes agricultural growth while protecting ecological barriers, adding 531.2 km² of cultivated land by 2050. However, this cultivated land expansion creates a water demand deficit (increasing to 4.87×108 m³), while maximum regional supply reaches only 0.16×108 m3, disrupting water balance. Consequently, the entire TRB will face water crises by 2050, with ≥46% of the area subjected to endangered (Level III) risk. Climate change and human activities jointly drive escalating water supply-demand risks. The root cause lies in persistent cultivated land expansion from intensive human activities, increasing irrigation demand and intensifying supply-demand conflicts. Findings emphasize deep integration of multi-method approaches within the risk framework to decipher land-eco-hydrological feedbacks and consider the complex interrelationships between climate, land, and water supply-demand. Deepening understanding of these linkages is vital for developing effective water scarcity mitigation strategies, providing crucial scientific support for policymakers and land

https://doi.org/10.5194/egusphere-2025-3089 Preprint. Discussion started: 2 July 2025 © Author(s) 2025. CC BY 4.0 License.

managers.





723 **Acknowledgements**724 This work was funded by the Major Science and Technology Project of Xinjiang
725 Autonomous Region (2023A02002-1) and Key Research and Development Plan of
726 Shaanxi Province (2023-YBNY-270). In addition, we would like to express our

gratitude to both the editors and reviewers for their efforts and suggestions.

727728





References

- Adem, E., Chaabani, A., Yilmaz, N., Boteva, S., Zhang, L., Elhag, M. 2024. Assessing the impacts of
 precipitation on water yield estimation in arid environments: Case study in the southwestern part of
 Saudi Arabia. Sustain Chem Pharm., 39, 101539, https://doi.org/10.1016/j.scp.2024.101539.
- Peña, A., Rosa, L., D'Odorico, P. 2020. Global food self-sufficiency in the 21st century under sustainable intensification of agriculture. Environ Res Lett., 15(9), 095004, https://doi.org/10.1088/1748-9326/ab9388.
- Boakes, E. H., Dalin, C., Etard, A., Newbold, T. 2024. Impacts of the global food system on terrestrial
 biodiversity from land use and climate change. Nat Commun., 15, 5750,
 https://doi.org/10.1038/s41467-024-49999-z.
- Bosmans, J. H., van Beek, L. P., Sutanudjaja, E. H., Bierkens, M. F. 2017. Hydrological impacts of global
 land cover change and human water use. Hydrol. Earth Syst. Sci., 21, 5603-5626.
 https://doi.org/10.5194/hess-21-5603-2017.
- Budyko, M.I., Miller, D.H., 1974. Climate and life. Academic Press, New York, 6 (3), 461–463.
 https://doi.org/10.1016/0033-5894(67)90014-2.
- Cao, D., Wang, Y., Zang, L. 2024. Land reallocation and collective action in the commons: Application
 of social-ecological system framework with evidence from rural China. Land Use Policy., 144,
 107267, https://doi.org/10.1016/j.landusepol.2024.107267.
- Caretta, A. M. M. A., Arfanuzzaman, R. B. M., Morgan, S. M. R. Kumar, M. Water. In: Climate Change
 2022: Impacts, Adaptation, and Vulnerability. Contribution of Working Group II to the Sixth
 Assessment Report of the Intergovernmental Panel on Climate Change (Cambridge Univ. Press,
 Cambridge and New York, 2022). https://www.ipcc.ch/report/ar6/wg2/.
- Carr, R., Kotz, M., Pichler, P. P., Weisz, H., Belmin, C., Wenz, L. 2024. Climate change to exacerbate the
 burden of water collection on women's welfare globally. Nat Clim Chang., 14(7), 700-706,
 https://doi.org/10.1038/s41558-024-02037-8.
- Chen, G., Zuo, D., Xu, Z., Wang, G., Han, Y., Peng, D., Pang, B., Abbaspour, K. C., Yang, H. 2024a.
 Changes in water conservation and possible causes in the Yellow River Basin of China during the
 recent four decades. J Hydrol., 637, 131314, https://doi.org/10.1016/j.jhydrol.2024.131314.
- 757 Chen, J., Pu, J., Li, J., Zhang, T. 2024b. Response of carbon-and water-use efficiency to climate change
 758 and human activities in China. Ecol Indic., 160, 111829,
 759 https://doi.org/10.1016/j.ecolind.2024.111829.
- Chen, M., Luo, Y., Shen, Y., Han, Z., Cui, Y. 2020. Driving force analysis of irrigation water consumption
 using principal component regression analysis. Agr Water Manage., 234, 106089,
 https://doi.org/10.1016/j.agwat.2020.106089.
- Chen, P., Wang, S., Liu, Y., Wang, Y., Wang, Y., Zhang, T., Zhang, H., Yao., Y., Song, J. 2023a. Water
 availability in China's oases decreased between 1987 and 2017. Earths Future., 11(4),
 e2022EF003340, https://doi.org/10.1029/2022EF003340.
- Chen, W., Wang, G., Gu, T., Fang, C., Pan, S., Zeng, J., Wu, J. 2023b. Simulating the impact of urban
 expansion on ecosystem services in Chinese urban agglomerations: A multi-scenario perspective.
 Environ Impact Asses., 103, 107275, https://doi.org/10.1016/j.eiar.2023.107275.
- Ding, R., Qin, Y., Li, T., Fu, G. 2024. Exploring spatiotemporal dynamics in temporal stability of soil
 carbon, nitrogen, phosphorus, and pH in Tibetan grasslands. Geoderma., 451, 117062,
 https://doi.org/10.1016/j.geoderma.2024.117062
- 772 Dolan, F., Lamontagne, J., Link, R., Hejazi, M., Reed, P., Edmonds, J. 2021. Evaluating the economic





- 773 impact of water scarcity in a changing world. Nat Commun., 12(1), 1-10 https://doi.org/10.1038/s41467-021-22194-0.
- Donohue, R.J., Roderick, M.L., McVicar, T.R., 2012. Roots, storms and soil pores: Incorporating key
 ecohydrological processes into Budyko's hydrological model. J Hydrol., 436, 35-50,
 https://doi.org/10.1016/j.jhydrol.2012.02.033.
- Duarte, H. F., Kim, J. B., Sun, G., McNulty, S. G., Xiao, J. 2024. Climate and vegetation change impacts
 on future conterminous United States water yield. J Hydrol., 639, 131472,
 https://doi.org/10.1016/j.jhydrol.2024.131472.
- Feng, Y., Zhang, W., Yu, J., Zhuo, R. 2025. Exploring nonlinear land use drivers and multi-scenario
 strategies for ecological impact mitigation: A case study of the Hohhot-Baotou-Ordos area, Inner
 Mongolia, China. Cities., 162, 105935, https://doi.org/10.1016/j.cities.2025.105935.
- Flörke, M., Schneider, C., McDonald, R. I. 2018. Water competition between cities and agriculture driven
 by climate change and urban growth. Nat Sustain., 1(1), 51-58, https://doi.org/10.1038/s41893-017 0006-8.
- Gaines, M. D., Tulbure, M. G., Perin, V., Composto, R., Tiwari, V. 2024. Projecting surface water area
 under different climate and development scenarios. Earths Future, 12(7), e2024EF004625,
 https://doi.org/10.1029/2024EF004625.
- Guo, Q., Yu, C., Xu, Z., Yang, Y., Wang, X. 2023. Impacts of climate and land-use changes on water
 yields: Similarities and differences among typical watersheds distributed throughout China. J
 Hydrol-Reg Stud., 45, 101294, https://doi.org/10.1016/j.ejrh.2022.101294.
- Guo, Y., Fang, G., Xu, Y. P., Tian, X., Xie, J. 2020. Identifying how future climate and land use/cover
 changes impact streamflow in Xinanjiang Basin, East China. Sci Total Environ., 710, 136275,
 https://doi.org/10.1016/j.scitotenv.2019.136275.
- Hamed, M. M., Sobh, M. T., Ali, Z., Nashwan, M. S., Shahid, S. 2024. Aridity shifts in the MENA region
 under the Paris Agreement climate change scenarios. Global Planet Change., 104483,
 https://doi.org/10.1016/j.gloplacha.2024.104483.
- Han, X., Kang, Y., Wan, S., Li, X. 2022. Effect of salinity on oleic sunflower (Helianthus annuus Linn.)
 under drip irrigation in arid area of Northwest China. Agr Water Manage., 259, 107267,
 https://doi.org/10.1016/j.agwat.2021.107267.
- Harifidy, R. Z., Hiroshi, I., Harivelo, R. Z. M., Jun, M., Kazuyoshi, S., Keiichi, M. 2024. Assessing future intra-basin water availability in madagascar: Accounting for climate change, population growth, and land use change. Water Res., 257, 121711, https://doi.org/10.1016/j.watres.2024.121711.
- He, C., Liu, Z., Wu, J., Pan, X., Fang, Z., Li, J., Bryan, B. A. 2021. Future global urban water scarcity and potential solutions. Nat Commun., 12, 4667, https://doi.org/10.1038/s41467-021-25026-3.
- He, X., Zhang, F., Zhou, T., Xu, Y., Xu, Y., Jim, C. Y., Johnson., B. A., Ma, X. 2025. Human activities
 dominated terrestrial productivity increase over the past 22 years in typical arid and semiarid regions
 of Xinjiang, China. Catena., 250, 108754, https://doi.org/10.1016/j.catena.2025.108754.
- Hu, Y., Cui, C., Liu, Z., Zhang, Y. 2025. Vegetation dynamics in Mainland Southeast Asia: Climate and
 anthropogenic influences. Land Use Policy., 153, 107546,
 https://doi.org/10.1016/j.landusepol.2025.107546.
- Huang, S., Krysanova, V., Zhai, J., Su, B. 2015. Impact of intensive irrigation activities on river discharge
 under agricultural scenarios in the semi-arid Aksu River basin, northwest China. Water Resour
 Manage., 29, 945-959, https://doi.org/10.1007/s11269-014-0853-2.
- 816 Huang, Y., Zheng, G., Li, X., Xiao, J., Xu, Z., Tian, P. 2024. Habitat quality evaluation and pattern





- simulation of coastal salt marsh wetlands. Sci Total Environ., 945, 174003,
- 818 https://doi.org/10.1016/j.scitotenv.2024.174003.
- 819 Huggins, X., Gleeson, T., Kummu, M., Zipper, S. C., Wada, Y., Troy, T. J., Famiglietti, J. S. 2022.
- Hotspots for social and ecological impacts from freshwater stress and storage loss. Nat Commun.,
- 821 13(1), 439, https://doi.org/10.1038/s41467-022-28029-w.
- 822 Jia, G, Hu, W.M., Zhang, B., Li, G., Shen, S.Y., Gao, Z.H., Li, Y., 2022. Assessing impacts of the
- Ecological Retreat project on water conservation in the Yellow River Basin. Sci Total Environ., 828,
- 824 154483, https://doi.org/10.1016/J. SCITOTENV.2022.154483.
- Jia, G., Li, C., Chen, X., Hu, Y., Chen, W., Kang, J. 2024. Impacts of Land Use and Climate Change on
- Water-Related Ecosystem Service Trade-offs in the Yangtze River Economic Belt. Ecosyst Health
- 827 Sust., 10, 0208, https://doi.org/10.34133/ehs.0208.
- Jones, E. R., Bierkens, M. F., van Vliet, M. T. 2024. Current and future global water scarcity intensifies
- when accounting for surface water quality. Nat Clim Chang., 14, 629-635,
- 830 https://doi.org/10.1038/s41558-024-02007-0.
- 831 Konapala, G., Mishra, A. K., Wada, Y., Mann, M. E. 2020. Climate change will affect global water
- availability through compounding changes in seasonal precipitation and evaporation. Nat Commun.,
- 833 11(1), 3044, https://doi.org/10.1038/s41467-020-16757-w.
- 834 Kulaixi, Z., Chen, Y., Li, Y., Wang, C. 2023. Dynamic evolution and scenario simulation of ecosystem
- 835 services under the impact of land-use change in an arid Inland River Basin in Xinjiang, China.
- 836 Remote Sens., 15(9), 2476, https://doi.org/10.3390/rs15092476.
- Li, C., Fu, B., Wang, S., Stringer, L. C., Wang, Y., Li, Z., Liu, Y., Zhou, W. 2021. Drivers and impacts of
- 838 changes in China's drylands. Nat Rev Earth Env., 2(12), 858-873, https://doi.org/10.1038/s43017-
- 839 021-00226-z.
- 840 Li, M., Wang, L., Singh, V. P., Chen, Y., Li, H., Li, T., Zhou, Z., Fu, Q. 2025a. Green and efficient fine
- control of regional irrigation water use coupled with crop growth-carbon emission processes. Eur J
- 842 Agron., 164, 127442, https://doi.org/10.1016/j.eja.2024.127442.
- 843 Li, S., Wei, W., Chen, Y., Duan, W., Fang, G. 2025b. TSWS: An observation-based streamflow dataset
- of Tianshan Mountains watersheds (1901–2019). Sci Data., 12, 708,
- 845 https://doi.org/10.1038/s41597-025-05046-0.
- 846 Li, Z., Fang, G., Chen, Y., Duan, W., Mukanov, Y. 2020. Agricultural water demands in Central Asia
- under 1.5 C and 2.0 C global warming. Agr Water Manage., 231, 106020.
- 848 https://doi.org/10.1016/j.agwat.2020.106020.
- 849 Liang, X., Guan, Q., Clarke, K.C., Liu, S., Wang, B., Yao, Y. 2021. Understanding the drivers of
- 850 sustainable land expansion using a patch-generating land use simulation (PLUS) model: a case study
- 851 in Wuhan, China. Comput Environ Urban Syst., 85, 101569,
- 852 https://doi.org/10.1016/j.compenvurbsys.2020.101569.
- 853 Liang, Y., Wen, Y., Meng, Y., Li, H., Song, L., Zhang, J., Ma, Z., Han, Y., Wang, Z. 2024. Effects of
- 854 biodegradable film types and drip irrigation amounts on maize growth and field carbon
- 855 sequestration in arid northwest China. Agr Water Manage., 299, 108894,
- 856 https://doi.org/10.1016/j.agwat.2024.108894/
- 857 Lipczynska-Kochany, E. 2018. Effect of climate change on humic substances and associated impacts on
- the quality of surface water and groundwater: A review. Sci Total Environ., 640, 1548-1565,
- https://doi.org/10.1016/j.scitotenv.2018.05.376.
- 860 Liu, C., Jiang, E., Qu, B., Li, L., Hao, L., Zhang, W. 2025a. Spatial-temporal evolution of economic-





- ecological benefits and their driving factors in Yellow River irrigation areas. Ecol Indic., 173, 113419, https://doi.org/10.1016/j.ecolind.2025.113419.
- Liu, J., Kuang, W., Zhang, Z., Xu, X., Qin, Y., Ning, J., Zhou, W., Zhang, S., Li, R., Yan, C., Wu, S., Shi,
 X., Jiang, N., Yu, D., Pan, X., Chi, W. 2014. Spatiotemporal characteristics, patterns, and causes of
 land-use changes in China since the late 1980s. J Geogr Sci., 24, 195-210,
 https://doi.org/10.1007/s11442-014-1082-6.
- Liu, T., Liu, H., Qi, Y. 2015. Built-up land expansion and cultivated land protection in urbanizing China:
 Insights from national land surveys, 1996–2006. Habitat Int., 46, 13-22,
 https://doi.org/10.1016/j.habitatint.2014.10.019.
- Liu, X., Liang, X., Li, X., Xu, X., Ou, J., Chen, Y., Li, S., Wang, S., Pei, F. 2017. A future land use
 simulation model (FLUS) for simulating multiple land use scenarios by coupling human and natural
 effects. Landscape Urban Plan., 168, 94-116, https://doi.org/10.1016/j.landurbplan.2017.09.019
- Liu, X., Liu, Y., Wang, Y., Liu, Z. 2022. Evaluating potential impacts of land use changes on water
 supply-demand under multiple development scenarios in dryland region. J Hydrol. 610, 127811,
 https://doi.org/10.1016/j.jhydrol.2022.127811.
- Liu, Y., Wang, X., Tan, M., Zhang, F., Li, X. 2025b. Impact of spatial transfer of farmland on the food water-GHG nexus in China during 2000–2020. Resour Conserv Recy., 221, 108390,
 https://doi.org/10.1016/j.resconrec.2025.108390.
- Lu, S., Shi, W. 2024a. Modeling the effects of the plastic-mulched cultivated land over the arid and semi-arid areas of China on the East Asian regional climate. J Hydrol. 634., 131123, https://doi.org/10.1016/j.jhydrol.2024.131123.
- Lu, Z., Li, W., Yue, R. 2024b. Investigation of the long-term supply-demand relationships of ecosystem
 services at multiple scales under SSP-RCP scenarios to promote ecological sustainability in China's
 largest city cluster. Sustain Cities Soc., 104, 105295, https://doi.org/10.1016/j.scs.2024.105295.
- Luo, Y., Wu, L., Wang, R., Wang, X., Du, B., Pang, S. 2025. Will vegetation restoration affect the supply demand relationship of water yield in an arid and semi-arid watershed? Sci Total Environ., 959,
 178292, https://doi.org/10.1016/j.scitotenv.2024.178292.
- Ma, F., Wang, H., Tzachor, A., Hidalgo, C. A., Schandl, H., Zhang, Y., Chen, W., Zhao, Y., Zhu, Y., Fu,
 B. 2025. The disparities and development trajectories of nations in achieving the sustainable development goals. Nat Commun., 16, 1107, https://doi.org/10.1038/s41467-025-56076-6.
- Ma, X., Zhang, P., Yang, L., Qi, Y., Liu, J., Liu, L., Fan, X., Hou, K. 2024. Assessing the relative
 contributions, combined effects and multiscale uncertainty of future land use and climate change on
 water-related ecosystem services in Southwest China using a novel integrated modelling framework.
 Sustain Cities Soc., 106, 105400, https://doi.org/10.1016/j.scs.2024.105400.
- Maron, M., Mitchell, M.G.E., Runting, R.K., Rhodes, J.R., Mace, G.M., Keith, D.A., Watson, J.E.M.,
 2017. Towards a threat assessment framework for ecosystem services. Trends Ecol Evol., 32 (4),
 240-248, https://doi.org/10.1016/j.tree.2016.12.011.
- McArthur, J. W., McCord, G. C. 2017. Fertilizing growth: Agricultural inputs and their effects in economic development. J Dev Econ., 127, 133-152, https://doi.org/10.1016/j.jdeveco.2017.02.007.
- Mekonnen, M. M., Hoekstra, A. Y. 2016. Four billion people facing severe water scarcity. Sci Adv., 2,
 e1500323, https://doi.org/10.1126/sciadv.1500323.
- 902 Mukherji, A. 2023. Climate Change 2023 Synthesis Report. https://www.ipcc.ch/report/sixth-903 assessment-report-cycle/.
- 904 Nourou, A. I. M., Garba, M., Grimsby, L. K., Aune, J. B. 2025. Manual or Motorized Postharvest





- Operations of Pearl Millet in Maradi, Niger: Effects on Time and Energy Use, Profitability, and Farmers' Perceptions. Food Energy Secur., 14(1), e70054, https://doi.org/10.1002/fes3.70054.
- Nuñez, J. A., Aguiar, S., Jobbágy, E. G., Jiménez, Y. G., Baldassini, P. 2024. Climate change and land
 cover effects on water yield in a subtropical watershed spanning the yungas-chaco transition of
 Argentina. J Environ Manage., 358, 120808. https://doi.org/10.1016/j.jenvman.2024.120808.
- O'Nill, B.C., Kriegler, E., Ebi, K.L., Kemp-Benedict, E., Riahi, K., Rothman, D.S., van Ruijven, B.J.,
 van Vuuren, D.P., Birkmann, J., Kok, K., Levy, M., Solecki, W., 2017. The roads ahead: narratives
 for shared socioeconomic pathways describing world futures in the 21st century. Glob Environ
 Change., 42, 169-180, https://doi.org/10.1016/j.gloenvcha.2015.01.004.
- O'Nill, B.C., Tebaldi, C., van Vuuren, D.P., Eyring, V., Friedlingstein, P., Hurrt, G., Knutti, R., Kriegler,
 E., Lamarque, J.F., Lowe, J., Meehl, G.A., Moss, R., Riahi, K., Sanderson, B.M., 2016. The scenario
 model intercomparison project (ScenarioMIP) for CMIP6. Geosci Model Dev., 9, 3461-3482,
 https://doi.org/10.5194/gmd-9-3461-2016.
- Ouyang, Y. 2025. Comparative analysis of evapotranspiration and water yield in basins of the Northern Gulf of America between the past and next 40 years. J Environ Manage., 381, 125157, https://doi.org/10.1016/j.jenvman.2025.125157.
- Patra, S., Shilky, Kumar, A., Saikia, P. 2023. Impact of land use systems and climate change on water
 resources: Indian perspectives. In Advances in Water Resource Planning and Sustainability (pp. 97 Singapore: Springer Nature Singapore. https://doi.org/10.1007/978-981-99-3660-1_10.
- Perez, N., Singh, V., Ringler, C., Xie, H., Zhu, T., Sutanudjaja, E. H., Villholth, K. G. 2024. Ending
 groundwater overdraft without affecting food security. Nat Sustain., 7, 1007-1017,
 https://doi.org/10.1038/s41893-024-01376-w.
- Piao, S., Friedlingstein, P., Ciais, P., de Noblet-Ducoudré, N., Labat, D., Zaehle, S. 2007. Changes in
 climate and land use have a larger direct impact than rising CO₂ on global river runoff trends. Proc
 Natl Acad Sci., 104, 15242-15247, https://doi.org/10.1073/pnas.0707213104.
- Qi, P., Li, B., Zhang, D., Xu, H., Zhang, G. 2025. Supply and demand of agricultural water resources
 under future saline-alkali land improvement. Agr Water Manage., 314, 109503,
 https://doi.org/10.1016/j.agwat.2025.109503.
- 933 Sharofiddinov, H., Islam, M., Kotani, K. 2024. How does the number of water users in a land reform 934 matter for water availability in agriculture? Agr Water Manage., 293, 108677, 935 https://doi.org/10.1016/j.agwat.2024.108677.
- Shi, Q., Gu, C. J., Xiao, C. 2023. Multiple scenarios analysis on land use simulation by coupling
 socioeconomic and ecological sustainability in Shanghai, China. Sustain Cities Soc., 95, 104578,
 https://doi.org/10.1016/j.scs.2023.104578.
- Shirmohammadi, B., Malekian, A., Salajegheh, A., Taheri, B., Azarnivand, H., Malek, Z., Verburg, P. H.
 2020. Impacts of future climate and land use change on water yield in a semiarid basin in Iran. Land
 Degrad Dev., 31(10), 1252-1264, https://doi.org/10.1002/ldr.3554.
- Song, K., Cheng, W., Wang, B., Xu, H. 2025. Impact of landform on Spatial-Temporal distribution and
 Scenario-Based prediction of carbon stocks in arid Regions: A Case study of Xinjiang. Catena., 250,
 108781, https://doi.org/10.1016/j.catena.2025.108781.
- Sun, J., Yang, Y., Qi, P., Zhang, G., Wu, Y. 2024. Development and application of a new water-carbon economy coupling model (WCECM) for optimal allocation of agricultural water and land resources.
 Agr Water Manage., 291, 108608, https://doi.org/10.1016/j.agwat.2023.108608.
- 948 Tan, X., Liu, B., Tan, X., Huang, Z., Fu, J. 2025. Combined impacts of climate change and human





- activities on blue and green water resources in a high-intensity development watershed. Hydrol.
 Earth Syst. Sci., 29, 427-445, https://doi.org/10.5194/hess-29-427-2025.
- Taylor, C., Blair, D., Keith, H., Lindenmayer, D. 2019. Modelling water yields in response to logging and representative climate futures. Sci Total Environ., 688, 890-902, https://doi.org/10.1016/j.scitotenv.2019.06.298.
- Tian, S., Wu, W., Chen, S., Li, Z., Li, K. 2025. Global Mismatch between Ecosystem Service Supply and
 Demand Driven by Climate Change and Human Activity. Environ. Sci Ecotechnol., 100573,
 https://doi.org/10.1016/j.ese.2025.100573.
- Valjarević, A., Popovici, C., Štilić, A., Radojković, M. 2022. Cloudiness and water from cloud seeding
 in connection with plants distribution in the Republic of Moldova. Appl Water Sci., 12(12), 262,
 https://doi.org/10.1007/s13201-022-01784-3.
- 960 Van Vliet, M. T. 2023. Complex interplay of water quality and water use affects water scarcity under 961 droughts and heatwaves. Nat Water., 1(11), 902-904. https://doi.org/10.1038/s44221-023-00158-6.
- Wang, M., Jiang, S., Ren, L., Cui, H., Yuan, S., Xu, J., Xu, C. Y. 2025. Attribution of streamflow and its
 seasonal variation to dual nature-society drivers using CMIP6 data and hydrological models. J
 Hydrol., 133314. https://doi.org/10.1016/j.jhydrol.2025.133314.
- Wang, X. J., Zhang, J. Y., Ali, M., Shahid, S., He, R. M., Xia, X. H., Jiang, Z. 2016. Impact of climate
 change on regional irrigation water demand in Baojixia irrigation district of China. Mitig Adapt
 Strat Gl., 21, 233-247, https://doi.org/10.1007/s11027-014-9594-z.
- Wang, Y., Hu, W., Sun, H., Zhao, Y., Zhang, P., Li, Z., An, Z. 2024a. Soil moisture decline in China's
 monsoon loess critical zone: More a result of land-use conversion than climate change. P Natl Acad
 Sci USA., 121(15), e2322127121. https://doi.org/10.1073/pnas.2322127121.
- Wang, Y., Li, M., Jin, G. 2024b. Optimizing spatial patterns of ecosystem services in the Chang-Ji-Tu
 region (China) through Bayesian Belief Network and multi-scenario land use simulation. Sci Total
 Environ., 917, 170424, https://doi.org/10.1016/j.scitotenv.2024.170424.
- 974 Wu, A., Wang, Z. 2025. Multi-scenario simulation and carbon storage assessment of land use in a multi-975 mountainous city. Land Use Policy, 153, 107529, https://doi.org/10.1016/j.landusepol.2025.107529.
- Wu, F., Tang, Q., Cui, J., Tian, L., Guo, R., Wang, L., Zheng, Z., Zhang, N., Zhang, Y., Lin, T. 2024.
 Deficit irrigation combined with a high planting density optimizes root and soil water–nitrogen distribution to enhance cotton productivity in arid regions. Field Crop Res., 317, 109524, https://doi.org/10.1016/j.fcr.2024.109524.
- 980 Yan, F., Shangguan, W., Zhang, J., Hu, B. 2020. Depth-to-bedrock map of China at a spatial resolution of 100 meters. Sci Data., 7(1), 2, https://doi.org/10.1038/s41597-019-0345-6.
- Yan, H., Xie, Z., Jia, B., Li, R., Wang, L., Tian, Y., You, Y. 2025. Impact of groundwater overextraction
 and agricultural irrigation on hydrological processes in an inland arid basin. J Hydrol., 653, 132770,
 https://doi.org/10.1016/j.jhydrol.2025.132770.
- Yao, J., Chen, Y., Guan, X., Zhao, Y., Chen, J., Mao, W. 2022. Recent climate and hydrological changes
 in a mountain-basin system in Xinjiang, China. Earth-Sci Rev., 226, 103957,
 https://doi.org/10.1016/j.earscirev.2022.103957.
- Yuan, C., Weng, Y., Xiong, K., Rong, L. 2024. Projections of Land Use Change and Water Supply—
 Demand Assessment Based on Climate Change and Socioeconomic Scenarios: A Case Study of
 Guizhou Province, China. Land, 13(2), 194. https://doi.org/10.3390/land13020194.
- Zeng, F., He, Q., Li, Y., Shi, W., Yang, R., Ma, M., Huang, W., Xiao, J., Yang, X., Di, D. 2024. Reduced
 runoff in the upper Yangtze River due to comparable contribution of anthropogenic and climate





- 993 changes. Earths Future., 12, e2023EF004028, https://doi.org/10.1029/2023EF004028.
- Zhang, H., Li, X., Luo, Y., Chen, L., Wang, M. 2024. Spatial heterogeneity and driving mechanisms of
 carbon storage in the urban agglomeration within complex terrain: Multi-scale analyses under
 localized SSP-RCP narratives. Sustain Cities Soc., 109, 105520,
 https://doi.org/10.1016/j.scs.2024.105520.
- Zhang, L., Hickel, K., Dawes, W.R., Chiew, F.H.S., Western, A.W., Briggs, P.R., 2004. A rational function
 approach for estimating mean annual evapotranspiration. Water Resour Res., 40 (2),
 https://doi.org/10.1029/2003WR002710.
- Zhang, M., Gao, Y., Ge, J. 2025a. Different responses of extreme and mean precipitation to land use and land cover changes. Npj Clim Atmos Sci., 8, 1-9. https://doi.org/10.1038/s41612-025-01049-1.
- Zhang, T., Shao, Q., Huang, H. 2025b. Understanding the efficiency and uncertainty of water supply
 service assessment based on the Budyko framework: A case study of the Yellow River Basin, China.
 Ecol Indic., 173, 113395, https://doi.org/10.1016/j.ecolind.2025.113395.
- Zhang, Z., Shan, Y., Tillotson, M. R., Ciais, P., Zhao, X., Zhao, D., Yang, H., Huo, J., Zeng, Z., Li, X.,
 Zheng, H., Cai, B., Wang, W., Kai, W., Li, G., Niu, G., Guan, D., Liu, J., Hao, Y. 2025c. Water-saving strategies across prefectures should target the manufacturing and agriculture sectors in China.
 Commun Earth Environ., 6(1), 1-18, https://doi.org/10.1038/s43247-025-02292-3.
- Zhao, Q., Chen, Y., Cuan, Y., Zhang, H., Li, W., Wan, S., Li, M. 2021. Application of ecosystem service
 bundles and tour experience in land use management: A case study of Xiaohuangshan Mountain
 (China). Remote Sens., 13(2), 242, https://doi.org/10.3390/rs13020242.
- Zhu, G., Qiu, D., Zhang, Z., Sang, L., Liu, Y., Wang, L., Zhao. K., Ma. H., Xu, Y., Wan, Q. 2021. Land-use changes lead to a decrease in carbon storage in arid region. China. Ecol Indic., 127, 107770, https://doi.org/10.1016/j.ecolind.2021.107770.
- Zhu, Y., Zhang, Y., Li, Y., Zheng, Z., Zhao, G., Sun, Y., Gao, J., Chen, Y., Zhang, J., Zhang, Y. 2023.
 Human activities further amplify the cooling effect of vegetation greening in Chinese drylands. Agr
 Forest Meteorol., 342, 109703, https://doi.org/10.1016/j.agrformet.2023.109703.
- 1019 Zhu, Y., Zheng, Z., Zhao, G., Zhu, J., Zhao, B., Sun, Y., Gao, J., Zhang, Y. 2025. Evapotranspiration 1020 increase is more sensitive to vegetation greening than to vegetation type conversion in arid and 1021 Global semi-arid regions of China. Planet Change., 244, 104634, 1022 https://doi.org/10.1016/j.gloplacha.2024.104634.
- Zhuang, D., Liu, J., Liu, M. 1999. Research activities on land-use/cover change in the past ten years in
 China using space technology. Chinese. J Geogr Sci., 9, 330-334, https://doi.org/10.1007/s11769 999-0006-3.